Biophysical Journal Volume 73 November 1997 2782–2790

Use of the Green Fluorescent Protein and Its Mutants in Quantitative Fluorescence Microscopy

George H. Patterson,* Susan M. Knobel,* Wallace D. Sharif,* Steven R. Kain,# and David W. Piston*
*Department of Molecular Physiology and Biophysics, Vanderbilt University, Nashville, Tennessee 37232, and #Clontech Laboratories, Palo Alto, California 94303 USA

ABSTRACT We have investigated properties relevant to quantitative imaging in living cells of five green fluorescent protein (GFP) variants that have been used extensively or are potentially useful. We measured the extinction coefficients, quantum yields, pH effects, photobleaching effects, and temperature-dependent chromophore formation of wtGFP, αGFP (F99S/M153T/V163A), S65T, EGFP (F64L/S65T), and a blue-shifted variant, EBFP (F64L/S65T/Y66H/Y145F). Absorbance and fluorescence spectroscopy showed little difference between the extinction coefficients and quantum yields of wtGFP and αGFP. In contrast, S65T and EGFP extinction coefficients made them both ~6-fold brighter than wtGFP when excited at 488 nm, and EBFP absorbed more strongly than the wtGFP when excited in the near-UV wavelength region, although it had a much lower quantum efficiency. When excited at 488 nm, the GFPs were all more resistant to photobleaching than fluorescein. However, the wtGFP and αGFP photobleaching patterns showed initial increases in fluorescence emission caused by photoconversion of the protein chromophore. The wtGFP fluorescence decreased more quickly when excited at 395 nm than 488 nm, but it was still more photostable than the EBFP when excited at this wavelength. The wtGFP and αGFP were quite stable over a broad pH range, but fluorescence of the other variants decreased rapidly below pH 7. When expressed in bacteria, chromophore formation in wtGFP and S65T was found to be less efficient at 37°C than at 28°C, but the other three variants showed little differences between 37°C and 28°C. In conclusion, no single GFP variant is ideal for every application, but each one offers advantages and disadvantages for quantitative imaging in living cells.

INTRODUCTION

The cloning of the green fluorescent protein (GFP) from the jellyfish *Aqueorea victoria* (Prasher et al., 1992) and subsequent expression in nonjellyfish systems (Chalfie et al., 1994; Inouye and Tsuji, 1994) introduced a new tool for the study of gene expression and protein localization. Because GFP does not require a unique factor from jellyfish to fold into the fluorescent structure, it is useful in many cell types (Heim et al., 1994; Inouye and Tsuji, 1994). GFP remains remarkably stable in the presence of many denaturants and proteases, as well as over a broad range of pH and temperature (Ward, 1981; Ward et al., 1982). In its native system, GFP emits green light through a strong energy transfer coupling mechanism with aequorin, a calcium-induced blue photoprotein (Morise et al., 1974). In heterologous systems, GFP displays a spectral pattern similar to that of fluorescein, which makes it easy to use in fluorescence microscopy. Most importantly, GFP is a cloned protein that can be used as an intrinsic intracellular reporter of gene expression, protein localization, and cell lineage in living tissue (Cubitt et al., 1995; Gerdes and Kaether, 1996; Niswender et al., 1995).

After GFP was cloned and expressed, genetic manipulations were performed in attempts to alter its fluorescent properties. Random and site-directed mutagenesis produced potentially useful mutants with single and multiple amino acid substitutions that exhibit excitation and emission spectra different from those of wtGFP. Among the most promising are the brighter mutants, such as S65T (Heim et al., 1995) and the similar GFPmut1 (Cormack et al., 1996), and mutants with shifted spectral peaks, such as P4 (Y66H) and P4–3 (Y66H/Y145F) (Heim and Tsien, 1996). Because the detection limit of wtGFP was determined to be ~1 μM over cellular autofluorescence (Niswender et al., 1995), the brighter mutants decrease this limit and allow the detection of lower levels of fluorescence (Cormack et al., 1996; Heim et al., 1995). Also useful are mutants with shifted absorbance and emission peaks, which allow the multiple labeling required for protein colocalization experiments. Spectrally shifted GFP mutants may also be useful for studying protein-protein interactions by fluorescence resonance energy transfer (FRET) methods (Herman, 1989). A blue-shifted double mutant, P4–3, has proved to be useful in two channel fluorescence experiments (Rizzuto et al., 1996), and a blue-shifted triple mutant, BFP5 (F64M/Y66H/V68I), has exhibited FRET in vitro when fused to a "green" GFP variant by a 20-amino acid linker (Mitra et al., 1996). A true "red fluorescent protein" has remained elusive, but a red-shifted mutant (T203/S65G/V68L/S72A) with limited spectral separation from other GFPs has been reported (Ormö et al., 1996). Another improvement of GFP for use in heterologous systems is the codon optimization of the GFP cDNAs (Chiu et al., 1996; Cormack et al., 1997; Haas et al.,

Received for publication 29 April 1997 and in final form 30 July 1997.

Address reprint requests to Dr. David W. Piston, Department of Molecular Physiology and Biophysics, 702 Light Hall, Vanderbilt University, Nashville, TN 37232. Tel.: 615-322-7030; Fax: 615-322-7236; E-mail: dave.piston@mcmail.vanderbilt.edu.

0006-3495/97/11/2782/09 $2.00

1996). In this work, we have used two human codon-optimized GFP mutants, EGFP (humanized version of GFPmut1) (Yang et al., 1996) and EBFP.

The mutants add flexibility in the use of GFP, but deviations from wild-type behavior may limit the usefulness of any particular mutant for a given application. To determine these limitations, we have measured the extinction coefficients, quantum yields, photobleaching rates, pH stabilities, and temperature-dependent folding efficiencies of five GFP variants: wtGFP (Chalfie et al., 1994), S65T (Heim et al., 1995), EGFP (F64L/S65T) (Yang et al., 1996), Stemmer cycle 3 mutant or αGFP (F99S/M153T/V163A) (Crameri et al., 1996), and EBFP (F64L/S65T/Y66H/Y145F) (Yang et al., manuscript submitted for publication). (Please note that an additional residue at the N-terminus of the protein caused the mutated residues for this protein to be originally reported as F100S/M154T/V164A. To avoid confusion, the mutation numbering scheme listed here corresponds to the other GFPs. To avoid the continuous use of a cumbersome name and because this mutant is available from Maxygen in the α + GFP cycle 3 mutant plasmid, the Stemmer cycle 3 mutant is denoted αGFP in this paper.)

Basic photophysical characteristics, such as the extinction coefficients and quantum yields, determine brightness and thus set the detection limit for the fluorophore. Photobleaching is also a limiting factor in fluorescence imaging that can complicate data analysis and interpretation. The wtGFP is reported to photobleach slowly, and we have quantitatively compared the photobleaching characteristics of each of the GFP variants mentioned above. The wtGFP also has a stable fluorescence signal over a relatively broad pH range, but the pH responses of the mutants have not been reported. We compared the fluorescence signals of these GFPs over a pH range of 4–9. Finally, because it is a potential problem with GFP that improper protein folding can lead to a nonfluorescent state and seriously decrease the GFP signal, we compared the temperature-dependent chromophore folding efficiencies of the GFPs.

MATERIALS AND METHODS

Plasmid constructs

The 2.9-kb plasmid pRSET A (Invitrogen Corporation, Carlsbad, CA) was used for the expression of histidine-tagged proteins. The cDNA of each GFP variant used here was subcloned in frame with the hexa-histidine tag sequence to produce an N-terminal His6 fusion protein. The S65T mutation was made by using the Kunkel method of site-directed mutagenesis (Sambrook et al., 1989a), with the TU#65 plasmid (Chalfie et al., 1994) as a template and an oligonucleotide, 5′-TGAACACCATAAGTGAAAGTAGTGACA-3′, as the annealing primer to give TU#65-S65T. The wtGFP and S65T were prepared by polymerase chain reaction amplification, with the N-terminal primer 5′-GCGGATCCATGAGTAAAGGAGAAGAACTTT-3′ containing a *Bam*HI site (underlined) and the C-terminal primer 5′-GTACCTGGAATTCTACGAATGCTA-3′ containing an *Eco*RI site (underlined) and the TU#65 and TU#65-S65T plasmids as templates. The amplification products were gel purified, digested with the restriction endonucleases *Bam*HI and *Eco*RI, and ligated into a similarly digested pRSET A to produce the protein expression plasmids pHisGFP and pHisS65T. The EGFP and the EBFP were prepared by PCR amplification by using the N-terminal primer 5′-GCGGATCCATGGTGAGCAAGGGCGAGGA-3′, containing a *Bam*HI site (underlined), and the C-terminal primer 5′-GCGAATTCTTACTTGTACAGCTCGTCCA-3′, containing an *Eco*RI site (underlined), and pEGFP-N1 and pEBFP (Clontech Laboratories, Palo Alto, CA), respectively, as templates. These amplification products were gel purified, digested with the restriction endonucleases *Bam*HI and *Eco*RI, and ligated into a similarly digested pRSET A to produce the pHis-EGFP and pHis-EBFP protein expression plasmids. pHis-αGFP was prepared by removing the *NheI*/*Eco*RI fragment containing the αGFP from α + GFP cycle 3 (Maxygen, Santa Clara, CA) by restriction endonuclease digestion and ligating it into an *NheI*/*Eco*RI-digested pRSETA plasmid. All pRSET plasmids were transformed into the *Escherichia coli* strain BL21 pLysS for protein expression. In this system, a high level of expression is driven by the T7 promoter in front of the His6-tagged proteins, and the T7 RNA polymerase is provided by the host BL21 strain (Studier et al., 1990). The pRSET and pLysS plasmids confer ampicillin and chloramphenicol resistance, respectively, on the expression strains.

Protein expression and purification

The His-tagged GFP variant proteins were expressed in *E. coli* grown at 28°C; for the temperature-dependence studies, the GFP variants were also grown and expressed at 37°C. Starter cultures were grown overnight in Terrific Broth (Sambrook et al., 1989b) containing 100 μg/ml ampicillin and 25 μg/ml chloramphenicol at 37°C. One-half of each starter culture was used to inoculate a 1-liter culture grown at 28°C, and the other half was used to inoculate a 1-liter culture at 37°C. These were incubated for 2 h at their respective temperatures, induced with 0.1 mM isopropylthio-β-D-galactopyranoside (IPTG), and grown for 5 h before harvesting by centrifugation. The cells were resuspended in sonication buffer (50 mM Na_2HPO_4, 300 mM NaCl, pH 8.0) and stored at −70°C until purification was continued. After thawing, the cells were lysed by incubation with lysozyme, followed by sonication. Insoluble debris was pelleted by centrifugation. The supernatant was incubated with Ni NTA agarose (Qiagen, Chatsworth, CA) in a 15-ml conical tube (Sarstedt, Newton, NC) for 1 h at room temperature on a rocker platform. The resin was pelleted by slow centrifugation, the supernatant was removed, and the resin was washed once with sonication buffer containing 10 mM imidazole. The wash was repeated once with sonication buffer containing 50 mM imidazole. The resin was packed into columns, and the proteins were eluted from the Ni NTA column with 1 ml of elution buffer (50 mM Na_2HPO_4, 300 mM NaCl, 200 mM imidazole, pH 8.0). Protein concentrations were determined by bicinchoninic acid (BCA) assay, and the purification efficiencies were determined by scanning densitometry of sodiumdodecyl sulfate gels stained with Coomassie brilliant blue. Only proteins that were purified to >95% homogeneity were used for experiments.

Spectroscopy

A Hewlett-Packard 8453 UV-visible spectrophotometer (Waldbronn, Germany) was used to perform absorbance measurements on the His-tagged GFPs in elution buffer. Extinction coefficients were calculated using Beer's law and the absorbance of 7 μM protein expressed at 28°C. Fluorescence excitation and emission measurements were performed on a SPEX 1681 Fluorolog spectrofluorometer with a 250-W xenon arc lamp (Edison, NJ). Quantum yield measurements were performed, using equal 488-nm optical densities of each variant and a fluorescein reference standard from Molecular Probes (Eugene, OR) in 0.1 M NaOH. Fluorescence emission profiles spanning 490–650 nm (excitation 488 nm) were summed and compared with the fluorescein standard (QY = 0.85) to give the absolute quantum yield of each "green" GFP (Morise et al., 1974). The EBFP quantum yield was determined in a similar manner, with the exceptions being that 390–550-nm emission (excitation 380 nm) spectra were collected, and an equal optical density at 380 nm of 1-aminoanthracene (QY = 0.61) (Berlman, 1971) in cyclohexane from Aldrich (Milwaukee,

WI) was used as the reference standard. For the pH stability measurements, the GFP variants were diluted to 100 nM in buffers containing 50 mM Na_2HPO_4, 50 mM sodium acetate, and 50 mM glycine, which were maintained at pH levels of 4, 5, 6, 7, 8, and 9. The fluorescence emission profiles were collected and summed as for the quantum yield measurements.

Microscopy

Laser scanning confocal microscopy was performed using a Bio-Rad MRC600 microscope with a 25× Plan Neofluar 0.8 NA glycerol immersion objective (Carl Zeiss, Thornwood, NY). The 488-nm line of an argon ion laser was used for excitation. The standard Bio-Rad BHS filter block with a Q498LP (Chroma Technology, Brattleboro, VT) was substituted for the original dichroic mirror. The detector pinhole was optimized for maximum S/N (Sandison et al., 1995).

Two-photon excitation microscopy was performed using a previously described instrument (Piston et al., 1995) with a Zeiss 40× Plan Neofluar 1.3 NA objective. The two-photon excitation spectra of the GFP variants studied overlay twice the one-photon spectra (Xu et al., 1996), allowing us to approximate 395-nm excitation by using two-photon excitation at 790 nm.

Photobleaching

Microdroplets of protein solutions were prepared in 1-octanol. These samples allowed us to photobleach the GFPs in vitro in a volume small enough to alleviate the problems of diffusion in the bleached region. To prepare the microdroplets, equimolar protein concentrations in elution buffer were mixed 1:9 with octanol by pipetting for 5 s and then vortexing for 20 s. Larger droplets were allowed to sediment for 10–15 s, and 15 μl of the solution was sealed between a slide and coverslip with paraffin. Round microdroplets ~50 μm in diameter were used for photobleaching experiments. The detected fluorescence signal from different GFP variants was normalized by adjusting the laser power with a variable neutral density filter (Newport Corp, Irvine, CA). Droplets were irradiated continuously while data points were taken once per minute. Mean pixel values of regions of interest encompassing the microdroplet image were used for comparisons. A mean pixel value of background outside the droplet was subtracted from each image. All images were analyzed with NIH Image software (National Institutes of Health, Bethesda, MD).

RESULTS

Spectroscopy

Proteins were expressed in *E. coli* at 28°C and purified to >95% homogeneity. After determining protein concentrations by BCA assay, equal amounts were analyzed by absorbance spectroscopy (Fig. 1 *A*). Both the wtGFP and the αGFP display two absorption peaks, a major peak at 397 nm and minor peak at 475 nm, whereas the S65T and EGFP each have one major peak at 489 nm. The αGFP and S65T spectra were omitted from Fig. 1, *A* and *B*, because they overlay those of wtGFP and EGFP, respectively. The blue-shifted EBFP has one peak at 380 nm. Also shown in Fig. 1 *A* is the absorption spectrum of denatured wtGFP (denoted deGFP), which was used for the studies of chromophore formation efficiency described below. The wtGFP extinction coefficient listed in Table 1 is within the range of measurements previously reported (Cubitt et al., 1995).

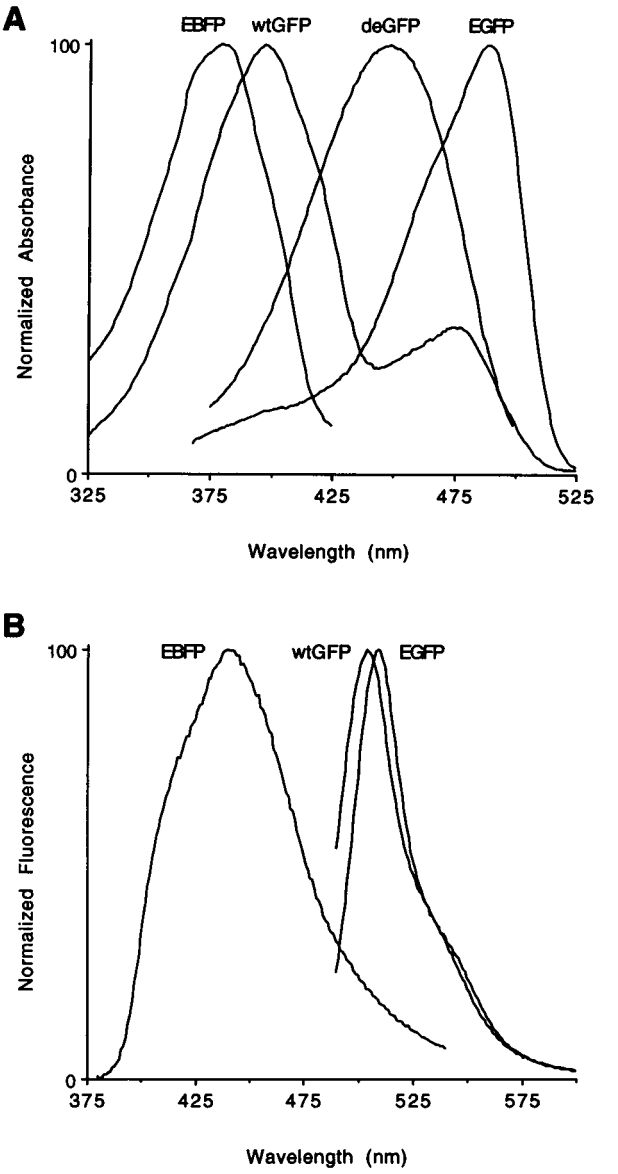

FIGURE 1 Absorption and fluorescence emission spectra from purified His-GFP variants. (*A*) The normalized absorption spectra of wtGFP, EGFP, and EBFP. The spectrum for αGFP overlays the wtGFP, and S65T overlays EGFP. When denatured in 0.2 M NaOH, all variants except for the EBFP exhibit a similar absorption peak at 448 nm (deGFP). (*B*) Fluorescence spectra of wtGFP, EGFP, and EBFP. Again, the spectrum for αGFP overlays the wtGFP and S65T overlays EGFP.

With the exception of the EBFP, the emission spectra were very similar (Fig. 1 *B*), and the maximum emission wavelengths were shifted less than 6 nm with respect to each other (Table 1). Using equal concentrations of protein in a spectrofluorometer, we found that both the S65T and EGFP mutants are both ~6 times brighter than the wtGFP when excited at 488 nm. The quantum yields of the GFP variants are listed in Table 1. The wtGFP QY measurement is also within the previously reported range (Cubitt et al., 1995). The EBFP emission spectrum, much like the absorbance, is dramatically blue-shifted with respect to wtGFP (Fig. 1 *B*).

TABLE 1 Summary of fluorescent protein photophysical properties

Protein	Absorbance peak (nm)		Extinction coefficient (M^{-1} cm^{-1})		Emission quantum peak (nm)	yield (%)#
	Major	Minor	Major*	Minor*		
wtGFP	397	475	25000 ± 3000	9500 ± 1500	504	79
S65T	489		55000 ± 5000		509	64
αGFP	397	475	30000 ± 2000	6500 ± 500	506	79
EGFP	489		53000 ± 4000		509	60
EBFP	380		31000 ± 2500		440	17

*Mean ± SD for each protein was determined from at least 12 measurements from 5 independent protein preparations.
#Mean for each protein was determined from four measurements. SD were <1%.

Effects of pH on GFP fluorescence

Fluorescence from native wtGFP has been found to be stable from pH 6 to pH 10 (Ward, 1981). In Fig. 2, we show the relative fluorescence emission of the variants at pH 4–9. The results for wtGFP are similar to the previous work over the corresponding pH range. The fluorescence of the wtGFP and αGFP proteins remains constant as the pH drops from 9 to 6 and decreases below pH 6. The fluorescence of the other three mutants begins to decrease below pH 7. The pH responses of αGFP and S65T were omitted from Fig. 2 because they closely overlay those of wtGFP and EGFP, respectively.

Photobleaching

We determined the relative photobleaching rates for the GFP variants by laser scanning confocal microscopy (LSCM) and two-photon excitation microscopy (TPEM).

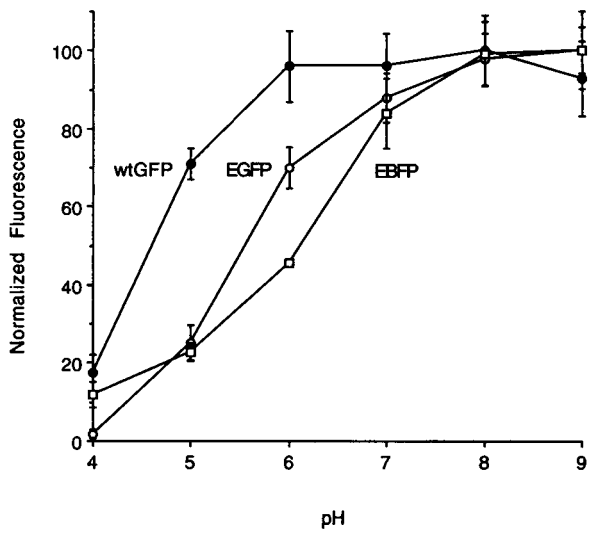

FIGURE 2 Effect of pH on GFP fluorescence. For wtGFP and EGFP, fluorescence was excited using 488 ± 1 nm and was collected from 490 to 650 nm. For EBFP, fluorescence was excited using 380 ± 1 nm and was collected from 390 to 550 nm. The maximum signal for each protein was normalized to 100. Standard errors were determined by using four measurements from two protein preparations. As with the absorption and fluorescence spectra, the pH dependence of αGFP is similar to that of wtGFP, and S65T is similar to EGFP.

LSCM photobleaching experiments were performed on wtGFP, S65T, αGFP, and EGFP, and TPEM experiments were performed on wtGFP, αGFP, and EBFP. The side view of a protein microdroplet compressed between a slide and coverslip (Fig. 3) shows that, despite the slight inward curvature along the edges, the droplets were cylindrical. When excited at 488 nm with an argon ion laser, the irradiation of the entire microdroplet results in a homogeneous mixture of photobleached and fluorescent molecules, negating any intradroplet diffusion effects on the LSCM photobleaching measurements. However, diffusion of GFP within the droplets is a factor in TPEM, where photobleaching occurs only within a 1-μm-thick focal plane, as discussed below.

To account for the different 488-nm extinction coefficients of the GFP variants, the laser power was adjusted with a neutral density filter to equalize the fluorescence signals. Keeping the detection variables (such as photomultiplier tube voltage, confocal aperture, and emission filters) constant allowed us to determine the relative photostabilities of the variants under normalized imaging conditions. Image analysis of the experiments yielded two distinct patterns (Fig. 4). The EGFP variant displayed a typical multiexponential photobleaching decay. In contrast, the wtGFP exhibited an initial increase in fluorescence followed by a rapid decrease. In these experiments, the αGFP and S65T patterns closely overlay the wtGFP and EGFP patterns, respectively, and were not included in the figure. Comparisons show that, when excited at 488 nm, all of these GFP variants photobleach at least five times more slowly than fluorescein.

We next investigated the initial rise of wtGFP and αGFP fluorescence during photobleaching. It was noted by Chalfie et al. (1994) that photobleaching of wtGFP with 340–390-nm light seemed to increase the fluorescence produced by 450–490 nm excitation. This was explained by other studies showing that continuous irradiation at 280 nm (Cubitt et al., 1995) or 398 nm (Chattoraj et al., 1996) induces a photoconversion in the chromophore, which decreases the 397-nm absorbance and increases the 475-nm absorbance. In our case, with irradiation at 488 nm, absorbance spectra of wtGFP indicate that a similar photoconversion occurs (Fig. 5). This photoconversion leads to the initial increase in fluorescence seen in Fig. 4.

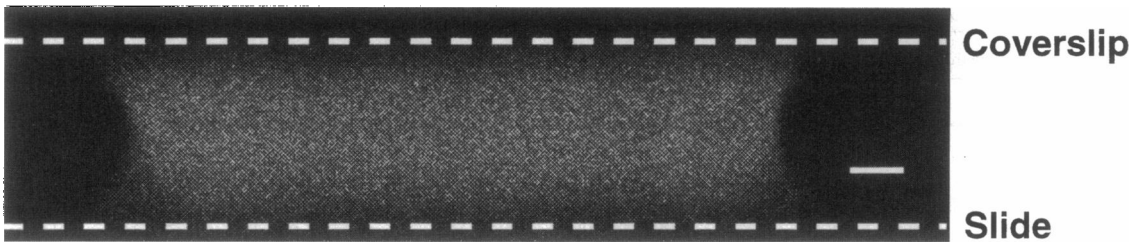

FIGURE 3 *X-Z* image showing the side view of a typical microdroplet containing His-wtGFP in 1-octanol that was used for photobleaching experiments. Despite the slight inward curvature of the sides, the droplet approximates a cylinder quite well. Scale bar is 5 μm.

We compared the mutant EBFP photobleaching properties with those of the wtGFP and αGFP by TPEM. Previous studies (Xu et al., 1996) have shown that the wtGFP and EBFP excitation spectra overlay twice their one-photon excitation spectra, so two-photon excitation with 790-nm light should approximate 395-nm excitation. Two-photon excitation wavelengths from 720 nm through 810 nm were tested, and the peak fluorescence intensity from wtGFP was indeed attained at 790 nm. The two photon photobleaching patterns in Fig. 4 reveal that the EBFP photobleaches much faster than the wtGFP. The photobleaching pattern of the wtGFP, when excited at the major absorbance peak, differs greatly from the 488-nm photobleaching because the photoconversion gives an extra "bleaching" factor. In this case, the photoconversion manifests itself as a faster decrease in fluorescence, because the absorbance at the major peak decreases as the minor peak absorbance increases (see Fig. 5). The αGFP photobleaching pattern was omitted because it directly overlays the wtGFP pattern.

As mentioned above, diffusion of GFP within the microdroplet affects the TPEM photobleaching measurements. Over an irradiation time of many minutes, the mixture of bleached and unbleached GFP molecules is homogeneous because a single GFP molecule can easily diffuse throughout the microdroplet in a time on the order of milliseconds (Luby-Phelps et al., 1986). Therefore, we can attempt to compare the LSCM results with those from TPEM. Because the droplets are on the order of 10 μm thick and the two-photon excitation occurs in a plane of $\sim$1 μm thickness, we would expect TPEM photobleaching rates to be $\sim$10 times slower than measured by LSCM for the same excitation rate. To compare the behavior of wtGFP under both LSCM and TPEM, we can examine the long time characteristics of the photobleaching curves, when the photoconversion process no longer dominates the observed

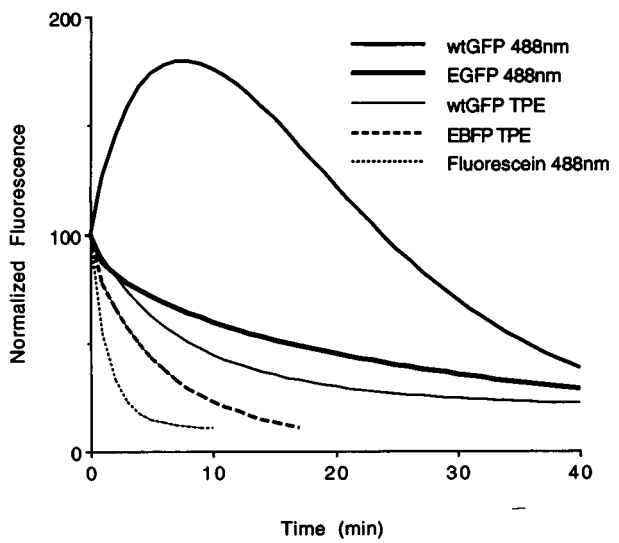

FIGURE 4 Time-resolved fluorescence changes during irradiation. Droplets containing 10 μM of a purified His-GFP variant were exposed continuously to scanned laser irradiation, as would be used in a confocal (488 nm) or a two-photon excitation (TPE at 790 nm) imaging experiment. Fluorescence from each GFP variant was initially equalized by adjusting the input laser power. Thus the curves represent the expected photobleaching-induced fluorescence decay that would be encountered from images with similar signal-to-noise ratios. The initial rise in wtGFP fluorescence is due to photoconversion (see Fig. 5). αGFP and S65T photobleaching were identical to wtGFP and EGFP, respectively. Each curve represents the average of 10 photobleaching experiments.

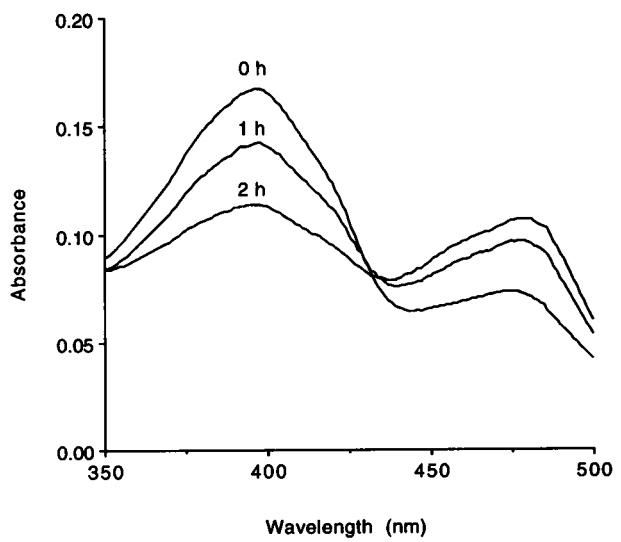

FIGURE 5 Photoconversion between the 475-nm and 397-nm absorption peaks by 488-nm irradiation. The sample was irradiated with 100 mW of 488-nm light from an Innova 310 ion laser (Coherent Laser Group, Santa Clara, CA) to produce the photoconversion. The decrease in 397-nm absorption is accompanied by a concomitant increase in 475-nm absorption. Because of experimental constraints, the times shown in Fig. 4 are not related to those in this figure.

behavior (after 20 min of irradiation). Least-squares fits show that the slow exponential decrease in wtGFP fluorescence excited at 488 nm has a rate constant (0.069 min^{-1}) that is ~10 times faster than the initial fluorescence decrease in wtGFP found by TPEM (0.010 min^{-1}). This suggests that the actual photobleaching rate of wtGFP excited in the near-UV is similar to its photobleaching rate when excited at 488 nm. However, when GFP is excited in the near-UV, apparently faster photobleaching arises from the photoconversion process.

Efficiency of chromophore formation

Potentially problematic in quantitative imaging of GFP is the expression of nonfluorescent GFP proteins. The requirement for incubations at temperatures less than 37°C to produce fluorescence signals in two earlier studies (Kaether and Gerdes, 1995; Ogawa et al., 1995) led to the proposal of a temperature effect on GFP folding. To test this proposal, the His-tagged GFP variants were expressed at both 28°C and 37°C and purified by affinity chromatography. Protein concentrations were determined by BCA protein assay and the denaturation method of Ward (1981). In the latter method, absorbances of the GFP variants all shift to one peak at 448 nm with a 44,100 M^{-1} cm^{-1} extinction coefficient when denatured in 0.2 M NaOH (Fig. 1 *A*; denatured GFP is denoted deGFP). This method directly measures chromophore concentration. Based on the ratio between concentrations determined by the BCA and denaturation assays, we estimated that roughly 25%, 30%, 95%, and 100% of the soluble wtGFP, S65T, EGFP, and αGFP, respectively, folded correctly when expressed at 37°C (Fig. 6). The GFP molecules that have not correctly formed chromophore appear to be permanently lost, as the percentage of active chromophore remains constant through denaturation/renaturation steps. When expressed at 28°C, the chromophores formed efficiently in all of the variants. The EBFP chromophore concentration could not be estimated by the Ward denaturation method. However, equal concentrations of EBFP (as determined by BCA assay) expressed at 28°C and 37°C had a similar 380-nm extinction coefficient, indicating that similar folding efficiencies were achieved at both temperatures.

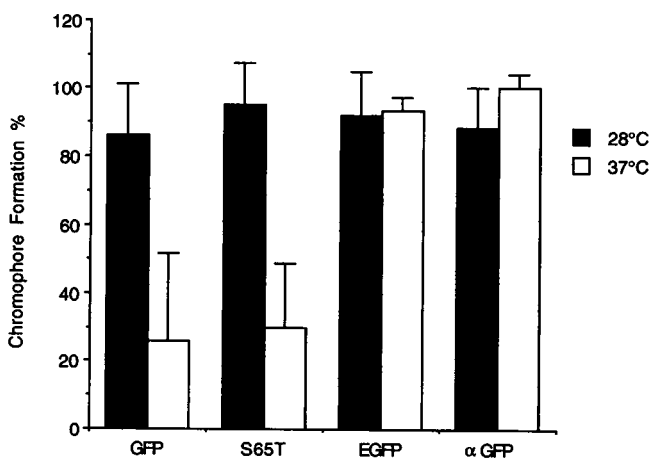

FIGURE 6 Temperature dependence of GFP chromophore formation in purified His-GFP variants. Chromophore formation efficiency was defined as the ratio of the concentration measured by denatured absorbance (concentration of GFP chromophore) and the concentration measured by BCA protein assay (concentration of GFP protein).

DISCUSSION

For accurate quantitation inside a living cell, both fluorescence and structural properties of GFP must be considered. Important fluorescence properties are the extinction coefficient and quantum yield, which determine the fluorophore brightness, and the photostability, which determines the fluorophore signal duration. Other important properties affecting the fluorescence of GFP, such as pH stability and chromophore formation, arise from the structural characteristics of the fluorescent protein. These are all intrinsic properties of the purified protein, and for many applications, the expression properties of the proteins are also important. We will discuss each of these properties in terms of advantages and disadvantages for imaging each of the GFP variants examined.

Of the current GFP derivatives, the S65T and EGFP will usually be the most useful for LSCM imaging experiments. Intrinsic brightness at 488-nm excitation enables detection of ~200 nM S65T and EGFP above typical cellular autofluorescence. This translates into a requirement of ~10,000 GFP molecules for accurate detection in the cytoplasm of a tissue culture cell. Of course, fewer molecules may be observed if they are spatially localized, such as on the plasma membrane or in an organelle. When exciting at 395 nm, as we did here with two-photon excitation, the wtGFP or αGFP gives a more intense signal and a better signal/autofluoresence ratio than when excited at 488 nm (Niswender et al., 1995). For near-UV excitation, EBFP absorbs better than the other reported blue mutants, P4 and P4–3 (Heim and Tsien, 1996), or any of the GFP variants studied here, but because of its low quantum yield, it exhibits only one-fourth the fluorescence of wtGFP. Although EBFP is potentially useful as a second label (as discussed below), for single-label experiments, the wtGFP and αGFP variants are better suited for near-UV excitation.

wtGFP and αGFP are the least desirable for use as a quantitative probe in LSCM, because an excitation-induced photoconversion in the chromophore complicates the data analysis. During the photoconversion, the absorbance at 397 nm decreases, whereas the 475-nm absorbance increases (Fig. 5) (Chattoraj et al., 1996; Cubitt et al., 1995). The photoconversion was previously reported to occur during irradiation at 280 nm (Cubitt et al., 1995) or 398 nm (Chattoraj et al., 1996). In contrast to the results of Cubitt et al. (1995), we found the photoconversion as an increase in fluorescence during excitation at 488 nm (Fig. 4) and con-

firmed the spectral change by absorbance spectroscopy (Fig. 5). In agreement with others (Chalfie et al., 1994; Chattoraj et al., 1996; Cubitt et al., 1995; Niswender et al., 1995), continuous irradiation at 395 nm decreases fluorescence emission much faster than 488-nm excitation (Fig. 4). But much of the loss in fluorescence at this wavelength is due to photoconversion rather than photobleaching, which implies that the photoconversion will complicate quantitation at 395-nm excitation as well. In our photobleaching experiments, we found that EGFP and S65T photobleach about twofold faster than wtGFP at 488 nm, but do not exhibit the photoconversion, which again suggests that they are most useful for LSCM. The fluorescence from the various GFPs was equalized by adjusting the excitation power, thus allowing direct comparisons of photostability per emitted fluorescent photon. Because the blue-shifted EBFP could not be directly compared with the other GFPs by using LSCM, it was compared with wtGFP and αGFP by two-photon excitation. We found that the EBFP photobleaches about twofold faster, which is similar to the P4–3 mutant observations reported by Rizzuto et al. (1996). The decreased photostability and the low quantum yields make the EBFP more difficult to use for near-UV excitation than the wtGFP or αGFP variants. The main strength of the EBFP, though, will be as a second label used in conjunction with a "green" GFP. The emission spectra (Fig. 1 *B*) show that the fluorescence from EBFP can easily be separated from the other GFP variants. In addition, the overlap between the EBFP emission and absorption of S65T or EGFP may be useful for fluorescence resonance energy transfer (FRET) experiments (Heim and Tsien, 1996; Mitra et al., 1996). A recently described "red-shifted" mutant (T203Y/S65G/V68L/S72A) may also be useful for double labeling and FRET experiments, but its properties have not been fully determined (Ormö et al., 1996). Although its emission maximum is shifted ~20 nm from that of S65T or EGFP, the fluorescence cannot be readily distinguished by eye.

The fluorescence of wtGFP is quite stable between pH 6 and pH 10, but decreases at lower pH and increases at higher pH (up to 12) (Ward, 1981). For cellular imaging, pH stability is most important when areas of the cell with acidic pH levels are targeted. For example, endocytic and exocytic pathway organelles, such as lysosomes, endosomes, coated vesicles, and secretory granules, maintain internal environments that can be as low as pH 4.6 (Mellman et al., 1986). At these lower pH levels, GFP signals may be very dim. In addition, because many acidic compartments are often involved in transport, their pH can change during normal cellular processes that would hinder accurate quantitation of GFP. We compared the pH dependence of the variants and found that αGFP again behaved as wtGFP. The wtGFP and the αGFP should be the most useful of the variants studied here for targeting to acidic cell compartments, because the EGFP, S65T, and EBFP mutants begin to lose a significant amount of fluorescence below pH 7 (Fig. 2).

Possibly the most difficult problem to overcome in making accurate measurements of GFP levels is improper GFP folding. In Heim et al. (1994), the *E. coli*-expressed wtGFP displayed two forms: a soluble, fluorescent form that exhibited native protein fluorescence characteristics and an insoluble, nonfluorescent form that targeted the inclusion bodies. This indicated that improper folding of the recombinant protein could occur, although it tended to be insoluble. Later studies with both wtGFP and S65T suggested an apparent temperature dependence of the fluorescence intensity in cultured cells (Kaether and Gerdes, 1995; Ogawa et al., 1995). Here we found a similar temperature dependence with wtGFP and S65T variants expressed at 28°C and 37°C (Fig. 6). Using methods to independently measure protein and chromophore concentrations, we found that the proteins expressed at 28°C were much brighter than proteins expressed at 37°C. Our results indicate that this is due to a permanent chromophore deformation rather than simple misfolding of the protein, because the decreased levels of fluorescence are retained after repeated denaturation-renaturation steps. Two variants, αGFP and EGFP, did not display this temperature dependence (Fig. 6), and may therefore be preferable to wtGFP and S65T, respectively. However, αGFP folded slightly, yet statistically significantly ($p < 0.025$) better at 37°C than at 28°C, a property that is also exhibited by another thermostable version named GFPA (Siemering et al., 1996). Both αGFP and GFPA have the V163A mutation, but because EGFP does not contain this mutation, thermostability is not exclusively dependent on this alanine mutation. The chromophore formation efficiencies are probably not dependent on the codon usage, because αGFP still retains the jellyfish codons, and similar experiments with a human codon-optimized S65T (data not shown) revealed no difference from the jellyfish S65T. Regardless, the ability of αGFP and EGFP to form chromophore efficiently at higher temperatures is particularly important for imaging living cells and organisms that may function correctly only at 37°C. For instance, incubation at 20°C has been used to increase fluorescence from S65T-transfected cells (Kaether and Gerdes, 1995), but to maintain mammalian physiology in development, gene expression, and transgenic experiments, low-temperature incubation is not always an option. Although the EBFP chromophore formation efficiency could not be measured directly, no obvious temperature dependence was found. Thus it appears that EBFP can be used effectively at 37°C.

The temperature-dependent chromophore formation has also complicated attempts to compare the brightness of GFP variants. Previously reported fluorescence increases of αGFP (42-fold) and EGFP (35-fold) over wtGFP have probably arisen from comparisons with improperly folded wtGFP, resulting in an overestimation of their brightness (Cormack et al., 1996; Crameri et al., 1996; Yang et al., 1996). In our work, we found that inefficient chromophore formation is often a problem with wtGFP and S65T. However, even at 37°C, some preparations of these variants exhibit relatively efficient chromophore formation. On the other hand, the preparations of αGFP and EGFP are rou-

tinely highly efficient. Only by using both the spectral and BCA assays for GFP concentration have we been able to consistently overcome chromophore formation problems in quantitative measurements.

We have compared the intrinsic protein properties of five GFP variants to determine their usefulness for quantitative imaging. When expression of GFP is driven by a strong promoter, optimization of expression (which we have not studied) may significantly increase the fluorescent signal. However, the big advantage of GFP is that it can be genetically fused to promoters or proteins, and expressed in a eukaryotic cell as an endogenous probe for gene expression or protein localization. In these cases, where GFP expression is defined by the strength of an endogenous promoter, the intrinsic protein properties described in this paper will likely determine the upper limit of the fluorescent signal. As with any fluorescent probe, GFP quantitation involves photophysical constraints, such as brightness and photobleaching. However, GFP has complications not encountered with other fluorescent probes, such as improper protein folding. Mutagenesis has improved GFP brightness, shifted its spectra, and helped to overcome many of the complications involved in its use, but has yet to provide the "perfect" GFP. Regardless, the currently available variants are adequate for performing a variety of quantitative imaging experiments in living cells.

We thank Prof. William W. Ward, Prof. Tony Weil, and Daniel G. González for helpful discussions and critical readings of the manuscript, and Stephanie C. Schroeder for discussions and assistance with site-directed mutagenesis.

These studies were supported by the Beckman Foundation Young Investigator Program and the Whitaker Foundation Biomedical Engineering Research Program. Confocal microscopy was performed at the Cell Imaging Shared Resource, supported by the Vanderbilt Cancer Center (CA68485) and the Diabetes Research and Training Center (DK20593).

REFERENCES

Berlman, I. B. 1971. Handbook of Fluorescence Spectra of Aromatic Molecules. Academic Press, New York.

Chalfie, M., Y. Tu, G. Euskirchen, W. W. Ward, and D. C. Prasher. 1994. Green fluorescent protein as a marker for gene expression. *Science.* 263:802–805.

Chattoraj, M., B. A. King, G. U. Bublitz, and S. G. Boxer. 1996. Ultra-fast excited state dynamics in green fluorescent protein: multiple states and proton transfer. *Proc. Natl. Acad. Sci. USA.* 93:8362–8367.

Chiu, W., Y. Niwa, W. Zeng, T. Hirano, H. Kobayashi, and J. Sheen. 1996. Engineered GFP as a vital reporter in plants. *Curr. Biol.* 6:325–330.

Cormack, B. P., G. Bertram, M. Egerton, N. A. R. Gow, S. Falkow, and A. J. P. Brown. 1997. Green fluorescent protein (GFP): a marker for gene expression in *Candida albicans*. *Microbiology.* 143(Part2): 303–311.

Cormack, B. P., R. H. Valdivia, and S. Falkow. 1996. FACS-optimized mutants of the green fluorescent protein (GFP). *Gene.* 173:33–38.

Crameri, A., E. A. Whitehorn, E. Tate, and W. P. C. Stemmer. 1996. Improved green fluorescent protein by molecular evolution using DNA shuffling. *Nature Biotechnol.* 14:315–319.

Cubitt, A. B., R. Heim, S. R. Adams, A. E. Boyd, L. A. Gross, and R. Y. Tsien. 1995. Understanding, improving and using green fluorescent proteins. *Trends Biochem. Sci.* 20:448–455.

Gerdes, H.-H., and C. Kaether. 1996. Green fluorescent protein: applications in biology. *FEBS Lett.* 389:44–47.

Haas, J., E.-C. Park, and B. Seed. 1996. Codon usage limitation in the expression of HIV-1 envelope glycoprotein. *Curr. Biol.* 6:315–324.

Heim, R., A. B. Cubitt, and R. Y. Tsien. 1995. Improved green fluorescence. *Nature.* 373:663–664.

Heim, R., D. C. Prasher, and R. Y. Tsien. 1994. Wavelength mutations and posttranslational autoxidation of green fluorescent protein. *Proc. Natl. Acad. Sci. USA.* 91:12501–12504.

Heim, R., and R. Y. Tsien. 1996. Engineering green fluorescent protein for improved brightness, longer wavelengths and fluorescence resonance energy transfer. *Curr. Biol.* 6:178–182.

Herman, B. 1989. Resonance energy transfer microscopy. *In* Fluorescence Microscopy of Living Cells in Culture. D. L. Taylor and Y. Wang, editors. Academic Press, San Diego, CA. 220–243.

Inouye, S., and F. I. Tsuji. 1994. *Aequorea* green fluorescent protein: expression of the gene and fluorescent characteristics of the recombinant protein. *FEBS Lett.* 341:277–280.

Kaether, C., and H. Gerdes. 1995. Visualization of protein transport along the secretory pathway using green fluorescent protein. *FEBS Lett.* 369: 267–271.

Luby-Phelps, K., D. L. Taylor, and F. Lanni. 1986. Probing the structure of the cytoplasm. *J. Cell Biol.* 102:2015–2022.

Mellman, I., R. Fuchs, and A. Helenius. 1986. Acidification of the endocytic and exocytic pathways. *Annu. Rev. Biochem.* 55:663–700.

Mitra, R. D., C. M. Silva, and D. C. Youvan. 1996. Fluorescence resonance energy transfer between blue-emitting and red-shifted excitation derivatives of the green fluorescent protein. *Gene.* 173:13–17.

Morise, H., O. Shimomura, F. H. Johnson, and J. Winant. 1974. Intermolecular energy transfer in the bioluminescent system of *Aquorea*. *Biochemistry.* 13:2656–2662.

Niswender, K. D., S. M. Blackman, L. Rohde, M. A. Magnuson, and D. W. Piston. 1995. Quantitative imaging of green fluorescent protein in cultured cells: comparison of microscopic techniques, use in fusion proteins and detection limits. *J. Microsc.* 180:109–116.

Ogawa, H., S. Inouye, F. I. Tsuji, K. Yasuda and K. Umesono. 1995. Localization, trafficking, and temperature-dependence of the Aequorea green fluorescent protein in cultured vertebrate cells. *Proc. Natl. Acad. Sci. USA.* 92:11899–11903.

Ormö, M., A. B. Cubitt, K. Kallio, L. A. Gross, R. Y. Tsien, and S. J. Remington. 1996. Crystal structure of the *Aequorea victoria* green fluorescent protein. *Science.* 273:1392–1395.

Piston, D. W., B. D. Bennett, and G. Ying. 1995. Imaging of cellular dynamics by two-photon excitation microscopy. *Microsc. Microanal.* 1:25–34.

Prasher, D. C., V. K. Eckenrode, W. W. Ward, F. G. Prendergast, and M. J. Cormier. 1992. Primary structure of the Aequorea victoria green-fluorescent protein. *Gene.* 111:229–233.

Rizzuto, R., M. Brini, F. D. Giorgi, R. Rossi, R. Heim, R. Y. Tsien, and T. Pozzan. 1996. Double labelling of subcellular structures with organelle-targeted GFP mutants in vivo. *Curr. Biol.* 6:183–188.

Sambrook, J., E. F. Fritsch, and T. Maniatis. 1989a. Appendix A: bacterial media, antibiotics, and bacterial strains. *In* Molecular Cloning: A Laboratory Manual. C. Nolan, editor. Cold Spring Harbor Laboratory, Cold Spring Harbor, NY. A.2.

Sambrook, J., E. F. Fritsch, and T. Maniatis. 1989b. Site-directed mutagensis of cloned DNA. *In* Molecular Cloning: A Laboratory Manual. C. Nolan, editor. Cold Spring Harbor Laboratory, Cold Spring Harbor, NY. 15.74–15.79.

Sandison, D. R., D. W. Piston, R. M. Williams and W. W. Webb. 1995. Resolution, background rejection, and signal-to-noise in widefield and confocal microscopy. *Appl. Optics.* 34:3576–3588.

Siemering, K. R., R. Golbik, R. Sever, and J. Haseloff. 1996. Mutations that suppress the thermosensitivity of green fluorescent protein. *Curr. Biol.* 6:1653–1663.

Studier, F. W., A. H. Rosenberg, J. J. Dunn and J. W. Dubendorff. 1990. Use of T7 RNA polymerase to direct expression of cloned genes. *Methods Enzymol.* D. V. Goeddel, editor. Academic Press, San Diego, CA. 60–89.

Ward, W. W. 1981. Properties of the coelenterate green-fluorescent protein. *In* Bioluminescence and Chemiluminescence. M. A. DeLuca and W. D. McElroy, editors. Academic Press, New York. 235–242.

Ward, W. W., H. J. Prentice, A. F. Roth, C. W. Cody, and S. C. Reeves. 1982. Spectral perturbations of the *Aequorea* green-fluorescent protein. *Photochem. Photobiol.* 35:803–808.

Xu, C., W. Zipfel, J. B. Shear, R. M. Williams, and W. W. Webb. 1996. Multiphoton fluorescence excitation: new spectral windows for nonlinear microscopy. *Proc. Natl. Acad. Sci. USA.* 93:10763–10768.

Yang, T.-T., L. Cheng, and S. R. Kain. 1996. Optimized codon usage and chromophore mutations provide enhanced sensitivity with the green fluorescent protein. *Nucleic Acids Res.* 24:4592–4593.